JACS
JOURNAL OF THE AMERICAN CHEMICAL SOCIETY
pubs.acs.org/JACS
Article

Molecular Cu Electrocatalyst Escalates Ambient Perfluorooctanoic Acid Degradation

Soumalya Sinha, Ashwin Chaturvedi, Rajeev K. Gautam, and Jianbing "Jimmy" Jiang*

Cite This: J. Am. Chem. Soc. 2023, 145, 27390−27396
Read Online

ABSTRACT: Groundwater reservoirs contaminated with perfluoroalkyl and polyfluoroalkyl substances (PFASs) need purifying remedies. Perfluorooctanoic acid (PFOA) is the most abundant PFAS in drinking water. Although different degradation strategies for PFOA have been explored, none of them disintegrates the PFOA backbone rapidly under mild conditions. Herein, we report a molecular copper electrocatalyst that assists in the degradation of PFOA up to 93% with a 99% defluorination rate within 4 h of cathodic controlled-current electrolysis. The current-normalized pseudo-first-order rate constant has been estimated to be quite high for PFOA decomposition (3.32 L h^{-1} A^{-1}), indicating its fast degradation at room temperature. Furthermore, comparatively, rapid decarboxylation over the first 2 h of electrolysis has been suggested to be the rate-determining step in PFOA degradation. The related Gibbs free energy of activation has been calculated as 22.6 kcal/mol based on the experimental data. In addition, we did not observe the formation of short-alkyl-chain PFASs as byproducts that are typically found in chain-shortening PFAS degradation routes. Instead, free fluoride (F^-), trifluoroacetate (CF_3COO^-), trifluoromethane (CF_3H), and tetrafluoromethane (CF_4) were detected as fragmented PFOA products along with the evolution of CO_2 using gas chromatography (GC), ion chromatography (IC), and gas chromatography−mass spectrometry (GC-MS) techniques, suggesting comprehensive cleavage of C−C bonds in PFOA. Hence, this study presents an effective method for the rapid degradation of PFOA into small ions/molecules.

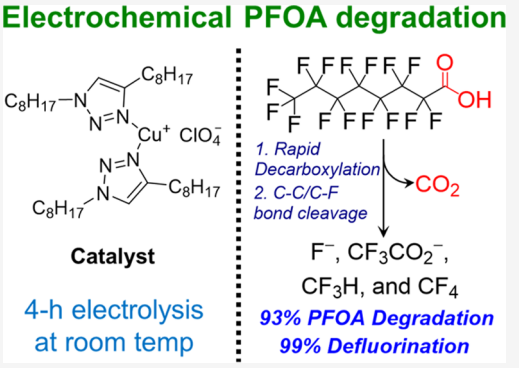

INTRODUCTION

Large-scale disposal of per- and polyfluoroalkyl substances (PFASs), typically owing to extensive application of surfactants in various industries, such as textiles, paper wastes, cosmetics, cookware, and in large-scale fracking operations, has led to severe environmental pollution, including groundwater contamination.[1−4] Perfluorooctanoic acid (PFOA) has been identified as the most common PFAS.[5−7] According to the CDC Fourth National Report on Human Exposure to Environmental Chemicals, all participants of the National Health and Nutrition Examination Survey were found to have more than 12 PFASs in their blood serum.[8] The high level of PFAS in the blood serum may increase cholesterol levels, cause hormone disruption, and increase the risk of various cancers.[9] Recent reports also indicate that high levels of PFAS in the blood could lead to poor response to vaccines, which may increase the risk of infectious diseases, such as the current COVID pandemic.[10,11] The U.S. Environmental Protection Agency is implementing new health advisories to regulate the PFAS level in drinking water.[12] Therefore, it is important to develop effective strategies to separate and degrade PFASs.

One of the challenges in PFOA degradation is cleaving highly stable C−F bonds.[5,13] It has been estimated that the bond dissociation energies (BDEs) of the terminal $-CF_3$ bonds are higher (117.8−123.4 kcal/mol) than those of the $-CF_2-$ bonds (106.4−113.6 kcal/mol) of PFOA (Figure 1A).[14,15] In general, PFOA degradation techniques, such as mechanochemical,[16−18] sonochemical,[19−21] electrochemical,[22−25] UV-induced additive-free degradation,[26,27] and photocatalytic approaches,[28−31] are known; however, most of these methods use harsh reaction conditions, such as high temperature, high pressure, utilization of toxic reagents, and high energy input. Furthermore, the production of undesired shorter-alkyl-chain PFASs is the common drawback of those strategies (Figure 1B).[15,28,32,33] Recently, Trang et al. showed that such shorter-alkyl-chain PFAS products could be avoided, and complete mineralization of PFOA is possible by decarboxylating PFOA in an aprotic solvent, followed by treating the decarboxylated PFOA with 30 equiv of NaOH at 40 °C for 24 h.[34] However, new strategies are still required for the rapid mineralization of PFOA under ambient conditions without using such a strong base.

In the area of reductive C−F bond cleavage, the electrochemical approach has been promising at ambient conditions,

Received: August 2, 2023
Revised: November 21, 2023
Accepted: November 22, 2023
Published: December 8, 2023

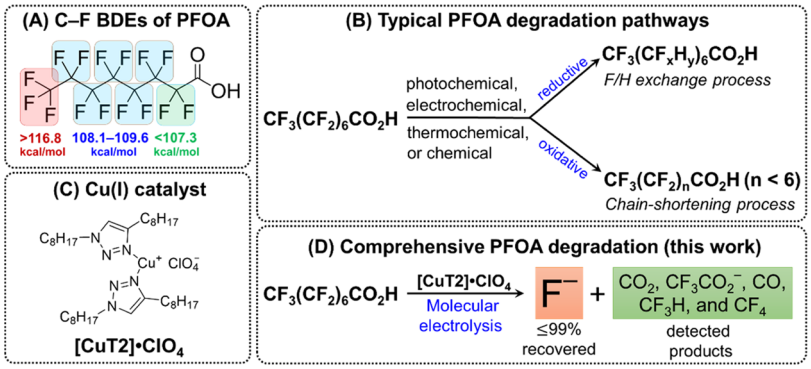

Figure 1. (A) Chemical structure of PFOA with C−F bond dissociation energies (BDEs) for $-CF_3$ and $-CF_2-$ groups. BDE values were adapted from ref 15. Copyright 2019 American Chemical Society. (B) Typical PFOA degradation processes, as reported in the literature (see refs 14, 15, 24, 28, 32, and 33). (C) Molecular Cu(I) electrocatalyst, $[\mathbf{CuT2}]^+$, studied in this work and (D) comprehensive PFOA degradation reaction performed by $[\mathbf{CuT2}]^+$ under homogeneous conditions in this work.

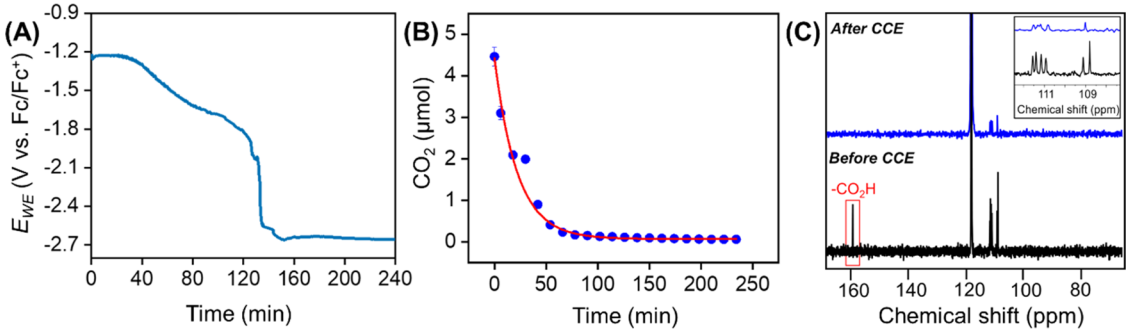

Figure 2. (A) Controlled-current electrolysis (CCE) of $[\mathbf{CuT2}]^+$ (1 mM) with 36 mM PFOA in the MeCN electrolyte at −1 mA. (B) Amount of CO_2 detected during the CCE. (C) Comparative ^{13}C NMR spectra (in CD_3CN) of pre- (black) and post-CCE catholytes (blue). Inset: ^{13}C signals for PFOA between 100 and 117 ppm (Figures S7 and S8 for full spectra).

but the substrate scopes are limited to fluoroarenes,[35−37] in which the C−F bond activation is easier than those in the PFAS.[38,39] Commonly, most of the electrochemical PFOA degradation processes treat PFOA oxidatively in the aqueous medium, and high PFOA degradation rates are achieved upon applying a high amount of current.[16−18] On the contrary, a recent report from Liu and co-workers revealed organic solvents, e.g., acetonitrile (MeCN), *N*,*N*-dimethylformamide (DMF), tetrahydrofuran (THF), etc., could be the better choice of media for decomposing PFOA reductively using rhodium/nickel cathodes, but their final products are also shorter-alkyl-chain PFASs.[40] Noteworthy, all of these electrochemical processes use solid electrode materials. In the area of electrocatalysis, molecular electrocatalysis provides flexible platforms for studying the structure−function relationship of the electrocatalytic reactions because of the synthetically easier tunability of the catalyst structure or the active site.[41,42] Surprisingly, no such molecular electrocatalyst for PFOA degradation is known yet that can rapidly decompose PFOA at room temperature without generating PFASs in the final products. Herein, we report a molecular Cu(I) electrocatalyst (Figure 1C) that degraded PFOA up to 93% in dry MeCN at room temperature under the application of a modest amount of a constant current (1−5 mA) for 4 h (Figure 1D).

EXPERIMENTAL SECTION

All chemical reagents were purchased from Sigma-Aldrich or Fisher Scientific and used as received without further purification. Solvents used in the synthesis and electrochemical studies were purified by passing through a column of activated alumina using an MBraun solvent purification system. The glassy carbon electrodes for cyclic voltammetry studies and carbon papers (GDS 2050) for controlled-current electrolysis were purchased from BASi and the Fuel Cell Store, respectively. Synthesis procedure, characterization techniques, and electrochemical methods are provided in the Supporting Information (see Sections SI-1−SI-12).

RESULTS AND DISCUSSION

We have previously reported that a molecular Cu(I) electrocatalyst bearing triazole-based ligands, $[\mathbf{CuT2}]\cdot\mathbf{PF_6}$, could activate C−Cl bonds with a high Faradaic efficiency (∼70%) for CH_2Cl_2-to-hydrocarbon conversion.[43] In the present study, we further explore the activities of such a Cu(I) complex toward C−F bond activation in PFOA by preparing $[\mathbf{CuT2}]\cdot\mathbf{ClO_4}$ (Figure 1C). We synthesized the $[\mathbf{CuT2}]\cdot\mathbf{ClO_4}$ complex (see Section SI-1 for the detailed synthesis) and characterized it by using ^1H nuclear magnetic resonance (NMR) and electrospray ionization mass spectrometry (ESI-MS). The ESI-MS and ^1H NMR data collected for $[\mathbf{CuT2}]\cdot\mathbf{ClO_4}$ matched with our previously reported $[\mathbf{CuT2}]^+$ complex, confirming the formation of the $[\mathbf{CuT2}]^+$ complex (see Figure S1A,B).[43]

Cyclic voltammogram (CV) of $[\mathbf{CuT2}]\cdot\mathbf{ClO_4}$ was first recorded after dissolving 1 mM of this complex in MeCN containing 0.1 M tetrabutylammonium perchlorate (TBA-ClO_4) as the supporting electrolyte (see Section SI-2). An irreversible cathodic wave at −1.33 V vs a ferrocene−ferrocenium (Fc/Fc^+) couple was observed (Figure S2A) owing to the reduction of ligands as the d-orbitals of Cu(I) are

https://doi.org/10.1021/jacs.3c08352
J. Am. Chem. Soc. 2023, 145, 27390−27396

filled. According to the density functional theory (DFT) calculation in our previous study, the electron added to $[\mathbf{CuT2}]^+$ likely delocalized on the two chelating triazole ligands.[43] However, the CVs of $[\mathbf{CuT2}]^+$ were also recorded at different scan rates. The peak currents at the irreversible reductive wave changed linearly with the square root of the scan rates (Figure S2B). Such a linear correlation in scan rate dependence studies confirms that it is a purely diffusion-controlled homogeneous process.[44]

To study the electrochemical PFOA degradation, we performed controlled-current electrolysis (CCE) in the MeCN electrolyte using a carbon paper working electrode in a N_2-sparged H-cell (see Section SI-3). The electrolyte solution containing 1 mM $[\mathbf{CuT2}]^+$ and 36 mM PFOA was subjected to CCE for 4 h under the reductively applied constant current of 1 mA. Under these CCE conditions, the potentials at the working electrode (E_{WE}) were initially around −1.2 V, which then shifted toward more negative potentials as the CCE progressed (Figure 2A). The headspace of the cathode compartment of the H-cell was analyzed at 6 min intervals using gas chromatography (GC, see Section SI-4), and the evolution of CO_2 was observed during CCE (Figure S3). The formation of CO_2 initially decreased exponentially during the first 2 h of electrolysis and then became constant at a low level near the baseline (Figure 2B), suggesting rapid decarboxylation of PFOA within the first 2 h of electrolysis. Trang et al. recently showed that PFOA could be chemically decarboxylated in polar aprotic solvents upon heating at 120 °C for 41 h.[34] Compared with this reported study, we observed much faster decarboxylation by treating PFOA electrochemically under mild conditions. To further confirm the complete decarboxylation process, we recorded fluorine-decoupled ^{13}C NMR spectra in CD_3CN for the pre- and post-CCE catholytes and observed that the carbon signal for the $-CO_2H$ functionality disappeared after CCE (Figure 2C). Notably, a small amount of CO was also observed and quantified using GC calibration curves (Figures S4 and S6), suggesting CO_2 reduction under the applied electrolysis conditions, which most likely utilized the carboxylic protons of PFOA.

Decarboxylation is the key step that initiates the subsequent C−F bond activation in PFOA degradation.[28,34] To investigate the C−F activation products, the post-CCE solution was further tested using ^{19}F NMR spectroscopy and ion chromatography (IC). The ^{19}F NMR spectrum revealed that after electrolysis (at −1 mA), the F-signal for a CF_2 group adjacent to the $-CO_2H$ group shifted from −119 to −116 ppm compared to that in the ^{19}F NMR spectrum of the pre-CCE solution (Figure 3A,B). The F-signal exhibited such a shift, possibly because the chemical environment of the $-CF_2-$ group (adjacent to $-CO_2H$) became different after decarboxylation. When $TBAPF_6$ was used as an internal standard for ^{19}F NMR studies (see Section SI-5), ∼79% of PFOA degraded when the CCE was conducted for 4 h in the presence of $[\mathbf{CuT2}]^+$. Furthermore, comparative ^{13}C NMR spectra for the pre-CCE and post-CCE solutions also exhibited the loss of carbon atoms after CCE, further supporting the decomposition of PFOA, especially the C−C bond cleavage in PFOA (Figures S7 and S8). The free F^- ions of the post-CCE solution obtained at −1 mA were quantified using IC (see Section SI-6). A calibration curve was first prepared for the F^- ions using four standard solutions of TBAF and fitted linearly (Figure S9). Using this calibration curve, 1.11 mmol of free F^- was detected in the same post-CCE solution (Figure S10),

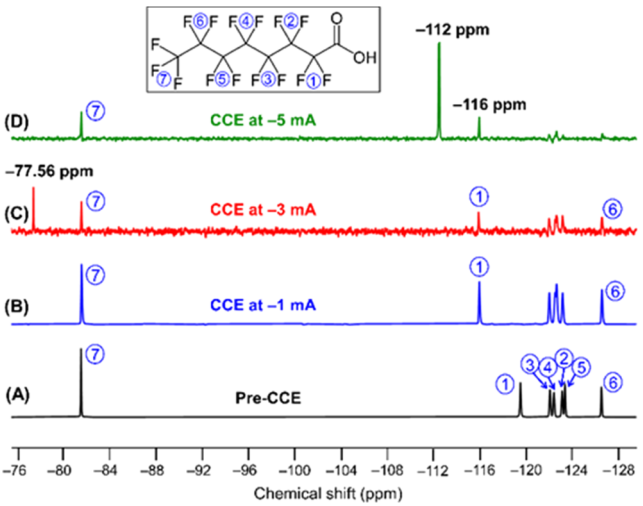

Figure 3. ^{19}F NMR of electrolytes containing $[\mathbf{CuT2}]^+$ and PFOA (A) before and after CCE at (B) −1 mA, (C) −3 mA, and (D) −5 mA of constant current (see Figures S15−S18 for full spectra).

corresponding to 51.4% of the overall defluorination rate of PFOA (see Section SI-7). Noteworthily, analysis of the post-CCE solution after 2 h of CCE showed only <5% degradation of PFOA with a negligible amount of free F^- ions in the postcatholyte solution. This indicates that defluorination of PFOA does not take place immediately after completion of the decarboxylation step. Therefore, it is important to perform an additional 2 h (at least) of CCE after the decarboxylation process to decompose the PFOA backbone for generating free F^- and other detectable products. Furthermore, the control experiment using a bare carbon electrode under identical CCE conditions but without $[\mathbf{CuT2}]^+$ facilitates the decarboxylation process (Figure S11), as shown by ^{19}F NMR (Figure S12). However, a negligible amount of F^- was observed in the IC (Figure S13), confirming that the bare carbon electrode is incapable of performing C−F bond cleavage. This control experiment highlights the importance of $[\mathbf{CuT2}]^+$ in PFOA mineralization processes. Moreover, another control CCE experiment (Figure S14) using $[\mathbf{CuT2}]^+$ but without PFOA did not show F^- formation, suggesting that F^- ions only are generated upon the degradation of PFOA.

The CCE experiments were further performed for $[\mathbf{CuT2}]^+$ and PFOA by applying a higher current (−3 mA, Figure S19) to enhance the rate of PFOA degradation and defluorination (%deF). The catholyte solution after CCE for 4 h exhibited a ^{19}F NMR spectrum similar to that shown in Figure 3B; however, the PFOA degraded by up to 91% and a new F-signal at −77.56 ppm was observed (Figure 3C). We compared this ^{19}F NMR spectrum with that of a standard sample of trifluoroacetic acid (Figure S20) and assigned the new signal at −77.56 ppm as the formation of $CF_3CO_2^-$. The headspace of the H-cell after CCE was analyzed using gas chromatography−mass spectrometry (GC-MS, see Section SI-8). The peaks at m/z 50, 51, 69, and 70 indicate the presence of CF_3H in the headspace and could be a potential PFOA degradation product (Figure S21). Furthermore, the IC data showed that % deF reached up to ∼84% when CCE was carried out at −3 mA (Figure S22). To investigate the correlation between the PFOA degradation rate with the concentration of PFOA, we have also tested six different concentrations of PFOA ranging from 12 to 72 mM by keeping the concentration of $[\mathbf{CuT2}]^+$

https://doi.org/10.1021/jacs.3c08352
J. Am. Chem. Soc. 2023, 145, 27390−27396

the same (1 mM) at −3 mA of applied current. In such experiments, we observed that the rate of PFOA degradation began to decrease when the PFOA concentration was >36 mM (see Table S1). It is speculated that such decrement in PFOA degradation rate could be because more substrate requires longer electrolysis duration (>4 h) to reach the maximum degradation limit.

We next performed identical CCE experiments using $[\mathbf{CuT2}]^+$ (1 mM) and PFOA (36 mM) at an even higher constant current, −5 mA, for 4 h (Figure S23). The results revealed the maximum degradation of PFOA up to 93% and 99% deF based on the IC data. Additionally, a more enhanced signal at −116 ppm and a new peak at −112 ppm were observed in the ^{19}F NMR spectra of the post-CCE solution (Figure 3D). To elucidate the enhancement of the F-signal at −116 ppm, we recorded the ^{19}F NMR spectrum at the halfway of CCE (2 h) and observed an increase in the F-signal at −116 ppm and an additional peak at −151 ppm (Figure S24). Next, we compared the ^{19}F NMR spectrum of TBAF·3H$_2$O (Figure S25) with that of $[\mathbf{CuT2}]^+$ and attributed the F-signals at −116 and −151 ppm to the formation of free F^- and HF_2^-, respectively.[45] As the CCE proceeded, more free fluoride began to accumulate, resulting in a more intense F-signal at −116 ppm, as confirmed by IC data (Figure S26). However, it is difficult to identify the PFOA-degraded product responsible for the fluorine signal at −112 ppm, because most of them are volatile and there is a lack of standard organofluorine complexes. The GC-MS data recorded from the headspace exhibited a signal at m/z 88, which hinted at the formation of CF_4 (Figure S27). Therefore, we propose that a new peak at −112 ppm appears, probably because of the generation of CF_4 by the reaction between CF_3^+ and free F^- in the solution. However, under a constant current of −5 mA, we achieved high %deF and PFOA mineralization of up to 99 and 93%, respectively. The comparative %deF and %PFOA degradations obtained at different applied currents are presented in Figure 4.

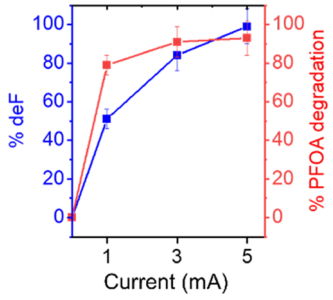

Figure 4. Degree of defluorination (%deF) and %PFOA decomposition at three different reductively applied currents: 1, 3, and 5 mA.

To gain more electrochemical insight, we calculated the Coulombic efficiencies for the defluorination processes at three different applied currents: −1, −3, and −5 mA (Figure 5A and Section SI-9) and obtained 3.7−4.08% of Coulombic efficiency (Table S2), which is ∼20,000 fold higher than that for the PFOA removal process from groundwater under 250 mA of applied current over 24 h.[24] However, these CE values are still low, indicating that additional electrons are required to cleave the bonds associated with the other PFOA degradation products before the C−F bond cleavage. Furthermore, we estimated the pseudo-first-order reaction rate constants (k) and their corresponding current-normalized values (k_n, see

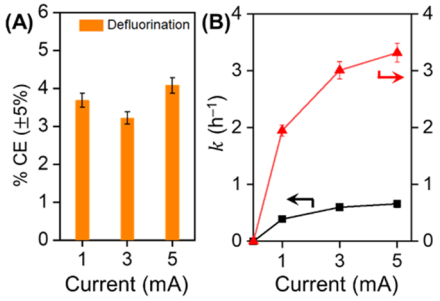

Figure 5. (A) Coulombic efficiencies (%CE), and (B) pseudo-first-order reaction rate constant, k, and current-normalized k_n vs applied current in CCE experiments.

Section SI-10) at the above-mentioned three applied currents (Figure 5B and Table S3). At −5 mA, k_n was 3.32 L h^{-1} A^{-1}, which is ∼14-fold higher than that of the reported rate for PFOA removal from groundwater.[24] We also estimated the Gibbs free energy of activation ($\Delta G^{\#}$) as 22.67 kcal/mol using the Eyring equation (see Section SI-11) based on four repeating CCE trials under identical electrochemical conditions (see Table S4). We think that such estimated $\Delta G^{\#}$ is associated with the rate-determining step, which is the initial decarboxylation step during PFOA degradation.[34]

To test the stability of $[\mathbf{CuT2}]^+$ during the CCE, we performed controlled-potential electrolysis (CPE) at different applied potentials, ranging from −1.2 to −2.6 V (Figure S28). These CPE experiments showed constant currents over time, and the current increased as the potentials were applied toward more negative potentials, indicating no such catalyst deactivation within the potential window of the CCE experiments. The long-term stability of $[\mathbf{CuT2}]^+$ was also studied upon performing CCE at −1 mA for 12 h (Figure S29), and scanning electron microscopy (SEM) images and energy-dispersive X-ray spectroscopy (EDX) data were collected for the pre- (Figures S30 and S31) and post-CCE (Figure S32) carbon working electrode surfaces. A negligible amount (∼0.54 wt %, Figure S33) of metallic Cu was observed on the carbon's surface. To further benchmark the stability of $[\mathbf{CuT2}]^+$, we also carried out a control CCE at −1 mA in the presence of PFOA under the above-mentioned electrochemical conditions using copper acetate ($Cu(OAc)_2$), instead of $[\mathbf{CuT2}]^+$. SEM images (Figure S34) and EDX data (Figure S35) collected for the carbon surface upon completing such a control CCE experiment revealed a large amount (>19.34 wt %) of metallic Cu deposition, suggesting that $Cu(OAc)_2$ was not comparatively stable during the CCE. Additionally, when IC data was recorded after the controlled experiment using a Cu^{2+} salt, no free fluoride ions were observed in the post-CCE solution (Figure S36). Therefore, it could be argued that $[\mathbf{CuT2}]^+$ does not undergo detectable demetalation during the electrolysis, as observed for Cu^{2+} salt ($Cu(OAc)_2$). The recovery of $[\mathbf{CuT2}]^+$ was attempted upon performing the CCE, but separating a small amount of catalyst (1 mM) from the solvent containing 100 equiv of electrolyte molecules is challenging as they both are soluble in most of the common organic solvents and might require more complicated treatments to isolate the Cu catalyst. Therefore, we considered the catalyst recovery out of the scope for this work.

We propose an outline of the PFOA degradation mechanism under the electrochemical conditions based on the experimental evidence (Figure 6). PFOA is initially deprotonated

https://doi.org/10.1021/jacs.3c08352
J. Am. Chem. Soc. 2023, 145, 27390−27396

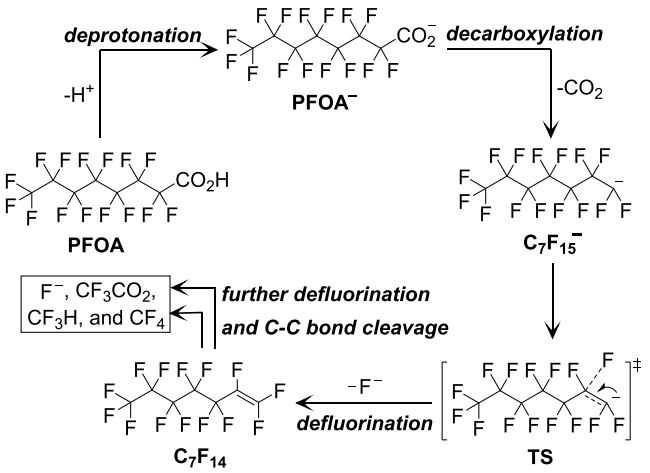

Figure 6. Plausible initial steps in the electrochemical PFOA degradation mechanism under the controlled-current electrolysis conditions. TS in the figure denotes the proposed transition state.

upon dissolution in MeCN to form **PFOA**$^-$, which then enters the chain-shortening process. The first step of such a chain-shortening process is decarboxylation, as confirmed by the rapid evolution of CO_2 during the first 2 h of CCE. The intermediate formed upon completing the decarboxylation process is $\mathbf{C_7F_{15}}^-$, which has been confirmed by detecting a signal at m/z 369.08 in the liquid chromatography−mass spectrometry (LC-MS) spectrum (see Figure S37). Furthermore, the LC-MS data of the same post-CCE solution also indicated the presence of **PFOA**$^-$ at m/z 413 (see Section SI-12 for the LC-MS sample preparation procedure). We believe that the $\mathbf{C_7F_{15}}^-$ intermediate undergoes a defluorination step to generate free F^- ions and becomes $\mathbf{C_7F_{14}}$ through a transition state **TS** (Figure 6), as also reported by Trang et al. in the nonaqueous solution.[34] Typically, a nucleophilic attack (such as adding excess NaOH) at the terminal double bond of $\mathbf{C_7F_{14}}$ further facilitates the PFOA degradation process to more comprehensive PFOA decomposition.[34] In our case, we believe electron-rich $[\mathbf{CuT2}]^+$ would interact with the $\mathbf{C_7F_{14}}$ intermediate and form more PFOA-degraded products through a series of C−C and C−F bond cleavage events.

CONCLUSIONS

In summary, we demonstrated the activity of a molecular Cu(I) electrocatalyst in PFOA degradation under a constant applied current (−1, −3, or −5 mA) for 4 h. The catalyst underwent PFOA degradation, which involves the cleavage of the C−C pathways. CO_2 was detected as a product of PFOA degradation. Additionally, we detected the formation of byproducts, such as free fluoride, trifluoroacetate, and trifluoromethane, using IC and GC-MS techniques. The maximum rate of defluorination was ∼99% throughout the CCE. Under −5 mA, >90% of PFOA degradation was achieved within 4 h. This study represents a rare example of a molecular electrocatalyst that rapidly degrades PFOA into small ions/molecules.

ASSOCIATED CONTENT

Supporting Information

The Supporting Information is available free of charge at https://pubs.acs.org/doi/10.1021/jacs.3c08352.

Experimental details, electrochemical and spectroscopy data (PDF)

AUTHOR INFORMATION

Corresponding Author

Jianbing "Jimmy" Jiang − *Department of Chemistry, University of Cincinnati, Cincinnati, Ohio 45221, United States;* orcid.org/0000-0002-7466-522X; Email: jianbing.jiang@uc.edu

Authors

Soumalya Sinha − *Department of Chemistry, University of Cincinnati, Cincinnati, Ohio 45221, United States;* orcid.org/0000-0002-6212-1102

Ashwin Chaturvedi − *Department of Chemistry, University of Cincinnati, Cincinnati, Ohio 45221, United States*

Rajeev K. Gautam − *Department of Chemistry, University of Cincinnati, Cincinnati, Ohio 45221, United States*

Complete contact information is available at: https://pubs.acs.org/10.1021/jacs.3c08352

Author Contributions

This manuscript was written through contributions of all authors.

Notes

The authors declare no competing financial interest.

ACKNOWLEDGMENTS

This work was supported by the National Science Foundation under Grant No. CBET-2051260. NMR experiments were performed on a Bruker AVANCE NEO 400 MHz NMR spectrometer funded by NSF-MRI Grant CHE-1726092. The authors acknowledge Dr. Alex Greenwood for his kind help in ^{19}F NMR data analysis.

REFERENCES

(1) Eriksson, U.; Kärrman, A. World-Wide Indoor Exposure to Polyfluoroalkyl Phosphate Esters (PAPs) and Other PFASs in Household Dust. *Environ. Sci. Technol.* **2015**, *49* (24), 14503−14511.

(2) Eriksson, U.; Haglund, P.; Kärrman, A. Contribution of Precursor Compounds to the Release of Per- and Polyfluoroalkyl Substances (PFASs) from Waste Water Treatment Plants (WWTPs). *J. Environ. Sci.* **2017**, *61*, 80−90.

(3) Shi, Y.; Vestergren, R.; Xu, L.; Song, X.; Niu, X.; Zhang, C.; Cai, Y. Characterizing Direct Emissions of Perfluoroalkyl Substances from Ongoing Fluoropolymer Production Sources: A Spatial Trend Study of Xiaoqing River, China. *Environ. Pollut.* **2015**, *206*, 104−112.

(4) Hogue, C. PFAS Used in Fracking Fluids in US, Report Says. *CEN Global Enterp.* **2021**, *99* (26), 17.

(5) Rahman, M. F.; Peldszus, S.; Anderson, W. B. Behaviour and Fate of Perfluoroalkyl and Polyfluoroalkyl Substances (PFASs) in Drinking Water Treatment: A Review. *Water Res.* **2014**, *50*, 318−340.

(6) Cui, J.; Gao, P.; Deng, Y. Destruction of Per- and Polyfluoroalkyl Substances (PFAS) with Advanced Reduction Processes (ARPs): A Critical Review. *Environ. Sci. Technol.* **2020**, *54* (7), 3752−3766.

(7) Xiao, F. Emerging Poly- and Perfluoroalkyl Substances in the Aquatic Environment: A Review of Current Literature. *Water Res.* **2017**, *124*, 482−495.

(8) Crinnion, W. J. The CDC Fourth National Report on Human Exposure to Environmental Chemicals: What It Tells Us About Our Toxic Burden and How It Assists Environmental Medicine Physicians. *Altern. Med. Rev.* **2010**, *15* (2), 101−108.

(9) Fenton, S. E.; Ducatman, A.; Boobis, A.; DeWitt, J. C.; Lau, C.; Ng, C.; Smith, J. S.; Roberts, S. M. Per- and Polyfluoroalkyl Substance Toxicity and Human Health Review: Current State of Knowledge and

Strategies for Informing Future Research. *Environ. Toxicol. Chem.* **2021**, *40* (3), 606−630.
(10) Grandjean, P.; Heilmann, C.; Weihe, P.; Nielsen, F.; Mogensen, U. B.; Timmermann, A.; Budtz-Jørgensen, E. Estimated Exposures to Perfluorinated Compounds in Infancy Predict Attenuated Vaccine Antibody Concentrations at Age 5-Years. *J. Immunotoxicol.* **2017**, *14* (1), 188−195.
(11) Looker, C.; Luster, M. I.; Calafat, A. M.; Johnson, V. J.; Burleson, G. R.; Burleson, F. G.; Fletcher, T. Influenza Vaccine Response in Adults Exposed to Perfluorooctanoate and Perfluorooctanesulfonate. *Toxicol. Sci.* **2014**, *138* (1), 76−88.
(12) US EPA. EPA Announces New Drinking Water Health Advisories for PFAS Chemicals, $1 Billion in Bipartisan Infrastructure Law Funding to Strengthen Health Protections. https://www.epa.gov/newsreleases/epa-announces-new-drinking-water-health-advisories-pfas-chemicals-1-billion-bipartisan (accessed September 12, 2022).
(13) Merino, N.; Qu, Y.; Deeb, R. A.; Hawley, E. L.; Hoffmann, M. R.; Mahendra, S. Degradation and Removal Methods for Perfluoroalkyl and Polyfluoroalkyl Substances in Water. *Environ. Eng. Sci.* **2016**, *33* (9), 615−649.
(14) Liu, J.; Van Hoomissen, D. J.; Liu, T.; Maizel, A.; Huo, X.; Fernández, S. R.; Ren, C.; Xiao, X.; Fang, Y.; Schaefer, C. E.; Higgins, C. P.; Vyas, S.; Strathmann, T. J. Reductive Defluorination of Branched Per- and Polyfluoroalkyl Substances with Cobalt Complex Catalysts. *Environ. Sci. Technol. Lett.* **2018**, *5* (5), 289−294.
(15) Bentel, M. J.; Yu, Y.; Xu, L.; Li, Z.; Wong, B. M.; Men, Y.; Liu, J. Defluorination of Per- and Polyfluoroalkyl Substances (PFASs) with Hydrated Electrons: Structural Dependence and Implications to PFAS Remediation and Management. *Environ. Sci. Technol.* **2019**, *53* (7), 3718−3728.
(16) Zhang, K.; Huang, J.; Yu, G.; Zhang, Q.; Deng, S.; Wang, B. Destruction of Perfluorooctane Sulfonate (PFOS) and Perfluorooctanoic Acid (PFOA) by Ball Milling. *Environ. Sci. Technol.* **2013**, *47* (12), 6471−6477.
(17) Ateia, M.; Skala, L. P.; Yang, A.; Dichtel, W. R. Product Analysis and Insight into the Mechanochemical Destruction of Anionic PFAS with Potassium Hydroxide. *J. Hazard. Mater. Adv.* **2021**, *3*, No. 100014.
(18) Lu, M.; Cagnetta, G.; Zhang, K.; Huang, J.; Yu, G. Mechanochemical Mineralization of "Very Persistent" Fluorocarbon Surfactants − 6:2 Fluorotelomer Sulfonate (6:2FTS) as an Example. *Sci. Rep.* **2017**, *7* (1), No. 17180.
(19) Moriwaki, H.; Takagi, Y.; Tanaka, M.; Tsuruho, K.; Okitsu, K.; Maeda, Y. Sonochemical Decomposition of Perfluorooctane Sulfonate and Perfluorooctanoic Acid. *Environ. Sci. Technol.* **2005**, *39* (9), 3388−3392.
(20) Vecitis, C. D.; Wang, Y.; Cheng, J.; Park, H.; Mader, B. T.; Hoffmann, M. R. Sonochemical Degradation of Perfluorooctanesulfonate in Aqueous Film-Forming Foams. *Environ. Sci. Technol.* **2010**, *44* (1), 432−438.
(21) Gole, V. L.; Fishgold, A.; Sierra-Alvarez, R.; Deymier, P.; Keswani, M. Treatment of Perfluorooctane Sulfonic Acid (PFOS) Using a Large-Scale Sonochemical Reactor. *Sep. Purif. Technol.* **2018**, *194*, 104−110.
(22) Zhuo, Q.; Deng, S.; Yang, B.; Huang, J.; Yu, G. Efficient Electrochemical Oxidation of Perfluorooctanoate Using a Ti/SnO_2-Sb-Bi Anode. *Environ. Sci. Technol.* **2011**, *45* (7), 2973−2979.
(23) Schaefer, C. E.; Andaya, C.; Urtiaga, A.; McKenzie, E. R.; Higgins, C. P. Electrochemical Treatment of Perfluorooctanoic Acid (PFOA) and Perfluorooctane Sulfonic Acid (PFOS) in Groundwater Impacted by Aqueous Film Forming Foams (AFFFs). *J. Hazard. Mater.* **2015**, *295*, 170−175.
(24) Schaefer, C. E.; Choyke, S.; Ferguson, P. L.; Andaya, C.; Burant, A.; Maizel, A.; Strathmann, T. J.; Higgins, C. P. Electrochemical Transformations of Perfluoroalkyl Acid (PFAA) Precursors and PFAAs in Groundwater Impacted with Aqueous Film Forming Foams. *Environ. Sci. Technol.* **2018**, *52* (18), 10689−10697.
(25) Lin, H.; Niu, J.; Xu, J.; Huang, H.; Li, D.; Yue, Z.; Feng, C. Highly Efficient and Mild Electrochemical Mineralization of Long-Chain Perfluorocarboxylic Acids (C9−C10) by Ti/SnO_2−Sb−Ce, Ti/SnO_2−Sb/Ce−PbO_2, and Ti/BDD Electrodes. *Environ. Sci. Technol.* **2013**, *47* (22), 13039−13046.
(26) Su, Y.; Rao, U.; Khor, C. M.; Jensen, M. G.; Teesch, L. M.; Wong, B. M.; Cwiertny, D. M.; Jassby, D. Potential-Driven Electron Transfer Lowers the Dissociation Energy of the C−F Bond and Facilitates Reductive Defluorination of Perfluorooctane Sulfonate (PFOS). *ACS Appl. Mater. Interfaces* **2019**, *11* (37), 33913−33922.
(27) Rao, U.; Su, Y.; Khor, C. M.; Jung, B.; Ma, S.; Cwiertny, D. M.; Wong, B. M.; Jassby, D. Structural Dependence of Reductive Defluorination of Linear PFAS Compounds in a UV/Electrochemical System. *Environ. Sci. Technol.* **2020**, *54* (17), 10668−10677.
(28) Wen, Y.; Rentería-Gómez, Á.; Day, G. S.; Smith, M. F.; Yan, T.-H.; Ozdemir, R. O. K.; Gutierrez, O.; Sharma, V. K.; Ma, X.; Zhou, H.-C. Integrated Photocatalytic Reduction and Oxidation of Perfluorooctanoic Acid by Metal−Organic Frameworks: Key Insights into the Degradation Mechanisms. *J. Am. Chem. Soc.* **2022**, *144* (26), 11840−11850.
(29) Roesch, P.; Vogel, C.; Simon, F.-G. Reductive Defluorination and Mechanochemical Decomposition of Per- and Polyfluoroalkyl Substances (PFASs): From Present Knowledge to Future Remediation Concepts. *Int. J. Environ. Res. Public Health* **2020**, *17* (19), 7242.
(30) Li, X.; Zhang, P.; Jin, L.; Shao, T.; Li, Z.; Cao, J. Efficient Photocatalytic Decomposition of Perfluorooctanoic Acid by Indium Oxide and Its Mechanism. *Environ. Sci. Technol.* **2012**, *46* (10), 5528−5534.
(31) Ochiai, T.; Iizuka, Y.; Nakata, K.; Murakami, T.; Tryk, D. A.; Koide, Y.; Morito, Y.; Fujishima, A. Efficient Decomposition of Perfluorocarboxylic Acids in Aqueous Suspensions of a TiO_2 Photocatalyst with Medium-Pressure Ultraviolet Lamp Irradiation under Atmospheric Pressure. *Ind. Eng. Chem. Res.* **2011**, *50* (19), 10943−10947.
(32) Fang, Y.; Ellis, A.; Choi, Y. J.; Boyer, T. H.; Higgins, C. P.; Schaefer, C. E.; Strathmann, T. J. Removal of Per- and Polyfluoroalkyl Substances (PFASs) in Aqueous Film-Forming Foam (AFFF) Using Ion-Exchange and Nonionic Resins. *Environ. Sci. Technol.* **2021**, *55* (8), 5001−5011.
(33) Tenorio, R.; Liu, J.; Xiao, X.; Maizel, A.; Higgins, C. P.; Schaefer, C. E.; Strathmann, T. J. Destruction of Per- and Polyfluoroalkyl Substances (PFASs) in Aqueous Film-Forming Foam (AFFF) with UV-Sulfite Photoreductive Treatment. *Environ. Sci. Technol.* **2020**, *54* (11), 6957−6967.
(34) Trang, B.; Li, Y.; Xue, X.-S.; Atei, M.; Houk, K. N.; Dichtel, W. R. Low-temperature mineralization of perfluorocarboxylic acids. *Science* **2022**, *377*, 839−845, DOI: 10.1126/science.abm8868.
(35) Xu, Y.; Ma, H.; Ge, T.; Chu, Y.; Ma, C.-A. Rhodium-Catalyzed Electrochemical Hydrodefluorination: A Mild Approach for the Degradation of Fluoroaromatic Pollutants. *Electrochem. Commun.* **2016**, *66*, 16−20.
(36) Wu, W.-B.; Li, M.-L.; Huang, J.-M. Electrochemical Hydrodefluorination of Fluoroaromatic Compounds. *Tetrahedron Lett.* **2015**, *56* (12), 1520−1523.
(37) Zhang, C. Z.; Lei, J. L.; Cai, S. M.; Tian, H.; Yang, M. Z. Study on the Electro-Reduction of Perfluorodecalin. *Chin. Chem. Lett.* **2002**, *13* (7), 666−669.
(38) Amii, H.; Uneyama, K. C−F Bond Activation in Organic Synthesis. *Chem. Rev.* **2009**, *109* (5), 2119−2183.
(39) Stahl, T.; Klare, H. F. T.; Oestreich, M. Main-Group Lewis Acids for C−F Bond Activation. *ACS Catal.* **2013**, *3* (7), 1578−1587.
(40) Zhu, J.; Chen, Y.; Gu, Y.; Ma, H.; Hu, M.; Gao, X.; Liu, T. Feasibility Study on the Electrochemical Reductive Decomposition of PFOA by a Rh/Ni Cathode. *J. Hazard. Mater.* **2022**, *422*, No. 126953.
(41) Sinha, S.; Williams, C. K.; Jiang, J. Outer-Coordination Sphere in Multi-H+/Multi-e−Molecular Electrocatalysis. *iScience* **2022**, *25* (1), No. 103628.
(42) Costentin, C.; Savéant, J.-M. Towards an Intelligent Design of Molecular Electrocatalysts. *Nat. Rev. Chem.* **2017**, *1* (11), No. 0087.

(43) Williams, C. K.; McCarver, G. A.; Lashgari, A.; Vogiatzis, K. D.; Jiang, J. Electrocatalytic Dechlorination of Dichloromethane in Water Using a Heterogenized Molecular Copper Complex. *Inorg. Chem.* **2021**, *60* (7), 4915−4923.
(44) Bard, A. J.; Faulkner, L. R. *Electrochemical Methods: Fundamentals and Applications*, 2nd ed.; Wiley: New York, 2001.
(45) Maity, K.; Panda, D. K.; Lochner, E.; Saha, S. Fluoride-Induced Reduction of Ag(I) Cation Leading to Formation of Silver Mirrors and Luminescent Ag-Nanoparticles. *J. Am. Chem. Soc.* **2015**, *137* (8), 2812−2815.

https://doi.org/10.1021/jacs.3c08352
J. Am. Chem. Soc. 2023, 145, 27390−27396